

## **Microfabricated mounts for high-throughput macromolecular cryocrystallography**

**R. E. Thorne, Z. Stum, J. Kmetko, K. O'Neill and R. Gillilan**

Copyright © International Union of Crystallography

Author(s) of this paper may load this reprint on their own web site provided that this cover page is retained. Republication of this article or its storage in electronic databases or the like is not permitted without prior permission in writing from the IUCr.

# Microfabricated mounts for high-throughput macromolecular cryocrystallography

R. E. Thorne,<sup>a\*</sup> Z. Stum,<sup>a</sup> J. Kmetko,<sup>a</sup> K. O'Neill<sup>a</sup> and R. Gillilan<sup>b</sup>Received 14 May 2003  
Accepted 18 August 2003<sup>a</sup>Laboratory of Atomic and Solid State Physics, Cornell University, Ithaca, NY 14853, USA, and  
<sup>b</sup>Macromolecular Diffraction Facility, Cornell High-Energy Synchrotron Source, Ithaca, NY 14853, USA. Correspondence e-mail: ret6@cornell.edu

A new approach is described for mounting microcrystals of biological macromolecules for cryocrystallography. The sample mounts are prepared by patterning thin polyimide films by standard microfabrication techniques. The patterned structures contain a small hole for the crystal connected to a larger hole *via* a drainage channel, allowing removal of excess liquid and easier manipulation in viscous solutions. These polyimide structures are wrapped around small metal rods. The resulting curvature increases their rigidity and allows a convenient scoop-like action in retrieving crystals. The polyimide contributes minimally to X-ray background and absorption, and can be treated to obtain desired hydrophobicity or hydrophilicity. The new mounts are fully compatible with existing automated sample-handling hardware for cryocrystallography. Their potential advantages include completely reproducible sample hole sizes to below 10  $\mu\text{m}$ ; accurate and reproducible sample positioning and good sample-to-mount contrast, simplifying alignment; more convenient manipulation of small crystals; easier removal of excess liquid and reduced background scatter; reduced thermal mass and more rapid flash-cooling; and easy design customization and mass production. They are especially well suited to data collection from the smaller crystals produced in high-throughput crystallization trials, and are suitable for automated crystal retrieval. They should be more generally useful for X-ray data collection from small organic and inorganic crystals of all types.

© 2003 International Union of Crystallography  
Printed in Great Britain – all rights reserved

## 1. Introduction

The development and application of cryocrystallographic techniques (Hope, 1988, 1990; Rodgers, 1994; Garman & Schneider, 1997; Parkin & Hope, 1998; Garman, 1999) has had a dramatic impact on the rate at which structures of biological macromolecules and macromolecular complexes can be solved. Much larger X-ray doses can be absorbed before radiation damage becomes significant, so that complete data sets can often be collected using a single crystal.

A variety of methods have been used to mount crystals for flash-cooling and cryocrystallographic data collection (Garman & Schneider, 1997). Early experiments attached crystals to the ends of glass fibers (Hope, 1990) or placed them on top of miniature glass spatulas (Hope *et al.*, 1989). The loop mounting method introduced by Teng (1990) and modified by using low X-ray absorption materials for the loop (Garman & Schneider, 1997) is now by far the most widely used mounting method. Loop cryomounts consist of a small (10–20  $\mu\text{m}$ ) diameter nylon (or metal) line that is twisted to form a loop and then threaded into a small hollow metal rod. This rod is then inserted into a metal or plastic goniometer-compatible base. Crystals are retrieved from the mother liquor, stabilizing solution or cryoprotectant solution by capturing them in the

loop. Crystals larger than the loop can rest on its surface, while smaller crystals can be trapped in the liquid film that spans the loop or else adhered to the side of the loop. Loop-mounted crystals are then flash-cooled by immersion in liquid nitrogen or propane or by insertion in a cold gas stream.

Loops provide convenient crystal manipulation. By holding crystals in the liquid film of the loop, potentially damaging contact with hard surfaces (such as those of alternative mounting tools) is minimized. The loop itself is flexible enough to make damage due to incidental contact less severe. Loops help minimize thermal mass and maximize surface area for heat transfer, increasing cooling rates and thus reducing cryoprotectant concentrations needed to prevent hexagonal ice formation within and surrounding the crystal (Kriminski *et al.*, 2003). For these reasons, loop-based mounts have been chosen as the standard for high-throughput automated cryocrystallography at synchrotron X-ray beamlines around the world.

However, loops have several problems. First, they are quite flexible, especially those made using 10  $\mu\text{m}$  diameter nylon line. Loops can bend under liquid and surface-tension forces during crystal retrieval from solution, and they can bend under the weight of the crystal and surrounding liquid once a crystal

is mounted. Because of their irregular aerodynamic profile they can bend and flutter under the drag forces of the cryostream, slightly broadening X-ray diffraction peaks for the lowest mosaicity crystals and reducing the maximum diffraction signal-to-noise achieved when crystal mosaicity and incident-beam divergence are matched.

Second, loops provide poor crystal positioning accuracy and reproducibility relative to the X-ray spindle axis. The loop shape for a given nominal loop diameter is irregular and irreproducible. The loop orientation relative to the metal post through which they are threaded is irregular, in part due to the twist of the nylon at their base needed to improve rigidity. Crystal positioning within the loop is irreproducible, especially for very small crystals. The crystal and the loop itself (which gains rigidity from frozen liquid) can shift during *in situ* crystal 'annealing' or 'tempering' protocols that raise the sample temperature near or above the melting point/glass transition of the surrounding solvent, necessitating crystal realignment in the X-ray beam (Yeh & Hol, 1998; Kriminski *et al.*, 2002).

Third, loops can trap significant liquid around the crystal. This liquid can be difficult to wick away, especially if the crystal is smaller than the loop's inner area. Remaining liquid increases background scattering, reducing diffraction signal-to-noise, and increases thermal mass, decreasing cooling rates. Moreover, surrounding liquid has different freezing properties and thermal expansion behavior than the crystal and can exert damaging forces during cooling. Frozen surrounding liquid also can make small (less than 50  $\mu\text{m}$ ) crystals difficult to image and align.

The limitations of loops are becoming increasingly apparent as crystallographers attempt structural studies using smaller and smaller crystals, made possible by continuing improvements in X-ray sources, optics and detectors. Initial crystal-

lization trials, especially those based on high-throughput robotic screening, usually yield very small crystals. Collecting X-ray data from these crystals can provide valuable feedback early in the growth-optimization process, and sometimes immediately yields useful structural information. Crystal size may remain small even after substantial optimization of crystal quality, especially in the case of macromolecular complexes and membrane proteins. Despite reduced signal-to-noise and increased radiation damage, smaller crystals may even be desirable because they flash-cool more rapidly and thus are easier to cryoprotect (Kriminski *et al.*, 2003); they can yield better diffraction data sets than larger crystals unless cryoprotection conditions for the latter are carefully optimized.

For crystals with sizes below 50  $\mu\text{m}$ , loops become extremely difficult to use. Flexibility constraints limit the minimum nylon diameter, which in turn limits the minimum inner loop diameter. Smaller crystals must often be held in a liquid meniscus of larger volume, reducing diffraction signal-to-noise and making alignment more difficult. Large liquid-to-crystal volume ratios also limit reductions in thermal mass and cooling times.

Recently, Protein Wave Corporation has marketed flat microfabricated polyimide films to replace glass coverslips for crystallization solution screening (<http://www.pro-wave.co.jp/>). Protein droplets are dispensed into one or more of several small holes in the film structure. If crystals appear, the portion of the film structure holding the crystals can be cut out and then mounted for X-ray diffraction. This approach has its merits, but the small drop volume within each hole may limit the probability that a crystal will nucleate (although there is anecdotal evidence that small drops promote nucleation), and any crystals that do grow will be small compared with the drop volume and hole diameter. Consequently, scattering from surrounding liquid will reduce the signal-to-noise ratio. Although polyimide (marketed under the trade name Kapton) has excellent X-ray transparency owing to its low density and the low atomic number of its constituent atoms, a flat film design requires thicknesses of roughly 25  $\mu\text{m}$  to give adequate rigidity during handling, flash-cooling and data collection, which may limit their usefulness for the smallest crystals. Cutting, mounting and reproducibly positioning the crystal-containing portion of the film for X-ray data collection are not straightforward.

Here we describe a microfabricated polyimide-film-based alternative to conventional loops that retains all of their advantages (including complete compatibility with existing and developing technologies for high-throughput cryocrystallography), but that resolves most if not all of their deficiencies in mounting very small crystals. Their potential advantages include completely reproducible sample 'loop' sizes below 10  $\mu\text{m}$ ; accurate and reproducible sample positioning and good sample-to-mount contrast; easier removal of excess liquid; reduced thermal mass and more rapid flash-cooling; reduced background scattering; and easy design customization. Since their fabrication utilizes standard methods from the microelectronics industry, they are ideally suited to low-cost mass production.

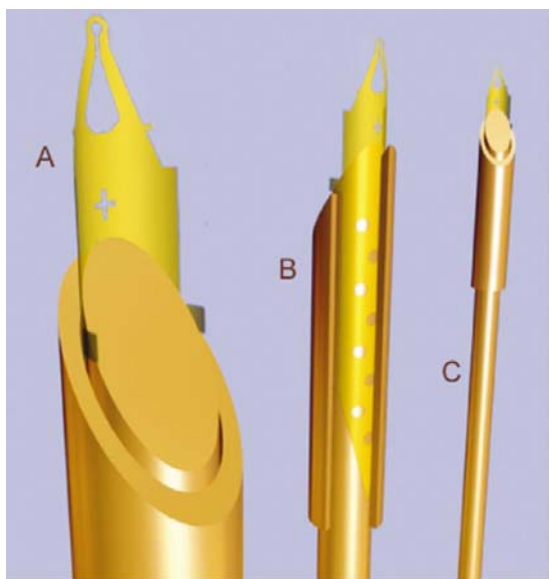


**Figure 1**  
Schematic illustration of the sample mounts, consisting of a patterned polyimide film (A), a retaining sleeve (B) and a metal rod (C). The beveling of the rod and sleeve at the end maximizes the viewing angle during crystal mounting.

## 2. Crystal mount design

Fig. 1 shows the basic features of our design, consisting of a microfabricated polyimide film (A) attached, for example, using a sleeve (B) to a beveled small-diameter metal post (C). This post can be inserted into standard plastic or metal magnetic goniometer head mounts such as those sold by Hampton Research, or into keyed variants of these allowing for higher precision alignment of the film and post relative to the goniometer head. The sleeve (B) and post (C) are beveled to maximize the viewing angle of the sample position, located at the tip of the polyimide film. The metal sleeve (B) rigidly attaches the film to the post and forces the film to conform to the post's curvature while allowing easy assembly. A small amount of glue is used to seal the area between sleeve and post and fix the sleeve relative to the post. The film can instead be glued or thermally bonded to the outside curvature of the post or to the inside curvature of a hollow post.

The curvature of the polyimide film induced by wrapping its base around the post dramatically increases its bending rigidity; a cylindrically curved piece of paper is much harder to bend than a flat one. This extra rigidity is crucial in allowing the film to be made very thin, minimizing background scatter from the polyimide and allowing film patterning to the small lateral dimensions required for mounting the smallest crystals. This curvature also produces a convenient scoop-like action in retrieving crystals.

Fig. 2 shows a typical pattern for the polyimide film. The small hole (D) at the narrow end plays the role of the loop in holding the crystal. This hole is connected *via* a channel (E) to a much larger opening (F). This structure allows a paper wick

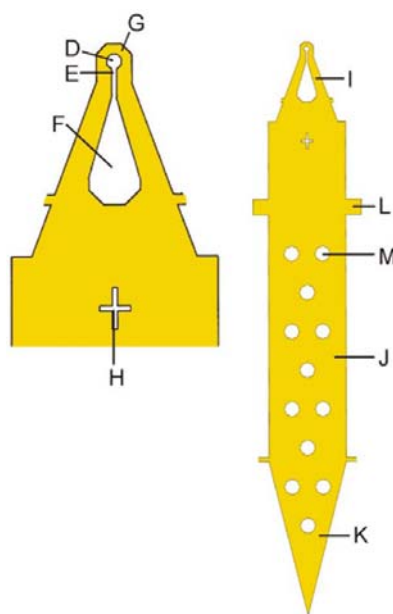


**Figure 2**

Polyimide film pattern. At the left is a close-up of the sample mounting end, and at the right is the overall patterned film, showing the extended tail that can be used for inserting and gluing the film to the inside of a hollow tube. The sample hole (D) is connected *via* a channel (E) to a larger opening into which a wick can be inserted for removal of excess liquid. H is a mark for automated alignment.

inserted into the larger opening to remove excess fluid from around the crystal *via* the channel, with little risk of touching the crystal. The larger opening also reduces the total area of polyimide and thus reduces the fluid resistance and flow disturbances caused as the mount is moved through a crystal-containing drop. The small fixed polyimide width (G) surrounding the sample opening reduces scattering from the polyimide (and any adsorbed fluid) when the plane of the film is oriented parallel to the X-ray beam. The small cross (H) centered beneath the sample hole (D) and opening (F) can be used to assist automated alignment. The overall triangular shape of the portion of the film (I) which extends beyond the post together with the post's tapered shape provides a good aerodynamic profile that minimizes sample 'flutter' in the gas cooling stream (relevant for lowest mosaicity crystals). The sample hole (D) can be customized to any shape so as to simplify mounting of, *e.g.* rod-shaped crystals. The film thickness can also be varied, *e.g.* to produce ridges surrounding the sample hole, to provide a stiffer base, or to modify the aerodynamics, but a uniform thickness provides more than adequate performance.

For ease of assembly, especially for attachment to the inside of a hollow post, an extended tail (J) with a tapered end (K) allows easy insertion of the film into the post. The small wings (L) stick out when the film is inserted and limit its travel into the post, providing reproducible positioning. For films to be attached to the outside of the post, a shorter broader tail with a square end can be used. In both cases, the tail can be perforated with small holes (M) to improve gluing strength. For the thinnest polyimide films, all right-angle cuts in the design, which are points of stress concentration, can be replaced with curves of finite radius to improve film robustness against tearing.

## 3. Fabrication of polyimide films

### 3.1. Process based on flexible circuit materials

To fabricate the patterned polyimide films we have used two different microfabrication processes, depending on the desired crystal hole size and film thickness. For holes larger than 50  $\mu\text{m}$ , a process based on the copper–polyimide–copper sheet material used for flexible electronic circuits can be employed. A silicon wafer is spin-coated with photoresist and a piece of this sheet material matching the wafer size is pressed on top using a piece of glass to ensure a flat surface. This assembly is then baked to cure the photoresist and firmly attach the copper–polyimide–copper to the wafer. A second layer of photoresist is then applied on top of the copper and the wafer baked a second time. This layer is exposed in a broad-band UV contact aligner through a chromium-glass mask containing the sample mount pattern (replicated to cover the wafer area) and then developed to remove the exposed photoresist. The pattern is etched into the top copper layer using ferric chloride, and is then etched into the polyimide using an  $\text{O}_2$ – $\text{CHF}_3$  gas plasma etch, after which the patterned copper–polyimide–copper film detaches from the wafer. The

patterned sheet is placed in a bath of Shipley 1165 to remove residual photoresist and then into a second ferric chloride bath to etch away all remaining copper on the top and bottom of the polyimide film.

The minimum feature (*e.g.* hole) size conveniently obtained by our process is limited to about 50  $\mu\text{m}$  by the non-vertical etch profiles and by the minimum copper (9  $\mu\text{m}$ ) and polyimide (25  $\mu\text{m}$ ) thicknesses of commercially available flexible circuit materials.

### 3.2. Process based on photodefinable polyimide

Our second process is based on photodefinable polyimide and can produce much smaller hole sizes. To begin, a 0.5  $\mu\text{m}$  silicon dioxide layer, to be used as a sacrificial layer during film lift-off, is deposited onto the surface of a clean silicon wafer. The wafer is spin-coated with positive-tone photoexposable PWDC1000 polyimide. Standard processes such as pre-coating with an adhesion promoter or pre-baking in a vapor-priming oven ensure good adhesion between the wafer and polyimide. After a brief bake, the polyimide is soft-contact exposed through a chromium-glass mask containing the mount's pattern, and then submerged in developer to remove the exposed polyimide. The remaining patterned polyimide is then cured in a nitrogen-atmosphere oven. Finally, the wafer is submerged in dilute HF to remove the sacrificial silicon dioxide layer, allowing the patterned polyimide film to float free of the wafer. This process is suitable for fabricating polyimide films with thicknesses of 5–15  $\mu\text{m}$ , which can then be patterned to a hole size of 10  $\mu\text{m}$ , suitable for mounting the smallest macromolecular crystals from which diffraction can currently be obtained. Fig. 3 shows a silicon wafer with a patterned polyimide film and a close-up of the sample mount structure before and after lift-off. In our preliminary work using 3 inch silicon wafers, we produce 130 sample mounts at a time. With 8 inch wafers this number can be increased to over 1000, making the individual mounts very inexpensive to produce. Other common microfabrication processes, such as

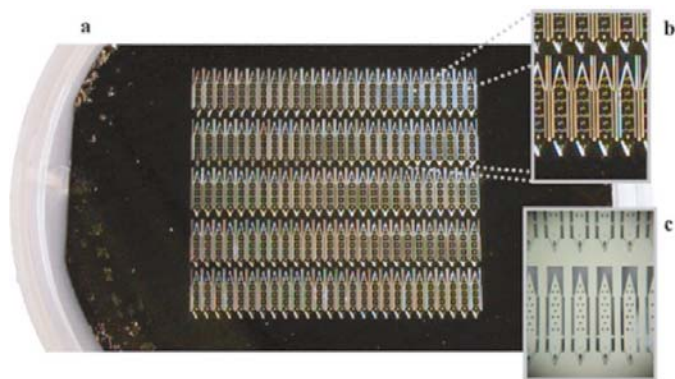


**Figure 3**  
(a) Three-inch silicon wafer covered by a polyimide film patterned with an array of 120 sample mounts. (b), (c) Close-ups showing the sample mounts (b) before and (c) after lift-off. The individual mounts are held in place in the repeating pattern by narrow and easily broken polyimide strips (also visible in Fig. 1 left).

contact printing and spray ('inkjet') printing, could also be used, especially for mounts with larger hole sizes.

### 3.3. Surface property modification

Polyimide is naturally hydrophobic. In this state, the sample mounts tend to repel mother liquor and can cause disturbance of protein-crystal-containing droplets. A broad variety of techniques have been developed to modify the surface properties of polyimide. To make our polyimide films hydrophilic, we briefly expose them to an oxygen gas plasma etch (Inagaki *et al.*, 1992) after lift-off and drying. This treatment minimizes drop disturbances and allows crystals to be easily retrieved. However, with practice untreated mounts appear to perform nearly as well and reduce excess liquid, and their hydrophobic properties may be more useful for drops containing detergents.

### 4. Mount evaluation and performance

Fig. 4 shows completed sample mounts using thick (25  $\mu\text{m}$ ) polyimide films fabricated using the copper–polyimide–copper process and thin (12  $\mu\text{m}$ ) films fabricated using the photo-

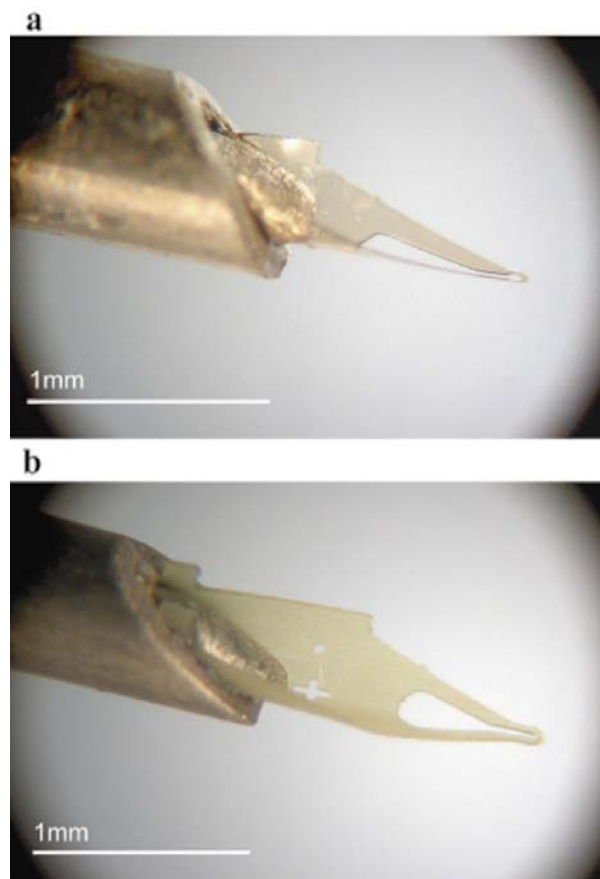


**Figure 4**  
Completed mounts attached to metal posts: (a) 12  $\mu\text{m}$  thick polyimide mounts fabricated using photodefinable polyimide; (b) 25  $\mu\text{m}$  thick mounts fabricated using copper–polyimide–copper flexible circuit material.

sensitive polyimide process. These images show the scoop-like character of the mounts.

Fig. 5 shows close-ups of the sample end of a thin-film mount with a 40  $\mu\text{m}$  sample opening. Fig. 5(a) shows a small tetragonal lysozyme crystal scooped into the opening from a paratone oil cryoprotectant, and (b) shows the crystal and mount after the oil has been wicked away. The very small amount of residual oil is sufficient to attach the crystal to the mount during flash-cooling. Fig. 5 also shows the good contrast

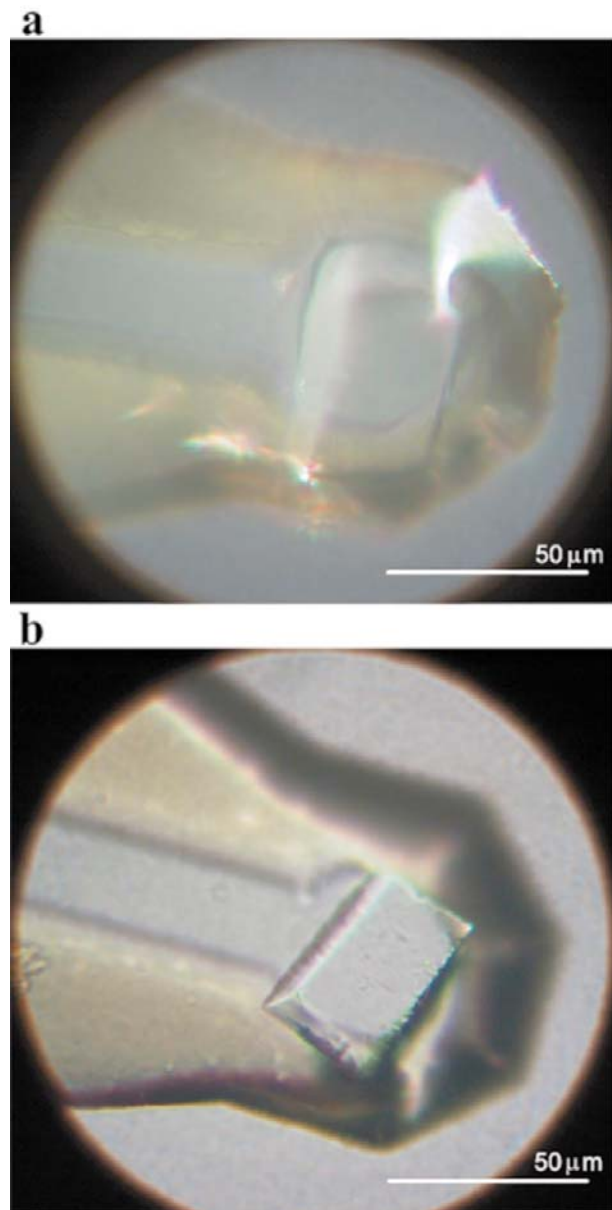


**Figure 5**

Photographs of a lysozyme crystal mounted in paratone oil over a 40  $\mu\text{m}$  hole (a) before and (b) after wicking away excess paratone oil by inserting a paper wick in the large opening (F in Fig. 1). Some care in choice and use of the wick is necessary to prevent the crystal from being drawn away with the excess fluid. Oil (or a humidified environment) prevents dehydration during mounting and handling of very small crystals.

between the yellow-gold polyimide film and the crystal, which makes locating and aligning the crystal easier. Mounts with hole diameters as small as 20  $\mu\text{m}$  have been used to retrieve and flash-cool a large number of crystals with sizes as small as 10  $\mu\text{m}$ .

Fig. 6 compares the diffuse X-ray background *versus* resolution  $2\sin(\theta)/\lambda$  produced by a 20  $\mu\text{m}$  nylon loop and a 9  $\mu\text{m}$  thick polyimide mount. The data were obtained on ESRF beamline ID-13 by illuminating the nylon and polyimide using a 12.7 keV X-ray beam focused to a 10  $\mu\text{m}$  spot. The more rigid polyimide mount provides much less background scatter, especially in the important 2–5  $\text{\AA}$  resolution range.

In general, with practice we find that the scoop-like action together with the reproducibility of the sample opening's size, shape and orientation make these mounts much easier to use than loops, especially for small crystals. These mounts can also be used for large crystals with sizes of hundreds of micrometers, provided that the thicker polyimide films are used. Because of the small volume of polyimide in the beam path and polyimide's low density and atomic number composition, its contribution to background scatter is small compared with that from disordered internal and external solvent, even for very small crystals. This volume can be reduced by optimizing the balance between film thickness (which determines bending rigidity) and the width of polyimide around the sample hole. The same basic design fabricated by a thin film process should be applicable down to sample holes of a few micrometers or less, provided the film thickness is reduced to account for the etch profile and the lateral mount dimensions are reduced to prevent buckling. For extremely small crystals the hole can be eliminated and a small curved solid area at the tip can be used to retrieve and support the crystal.

Another major advantage of these mounts is that they are much more rigid than loops. They remain rigid when

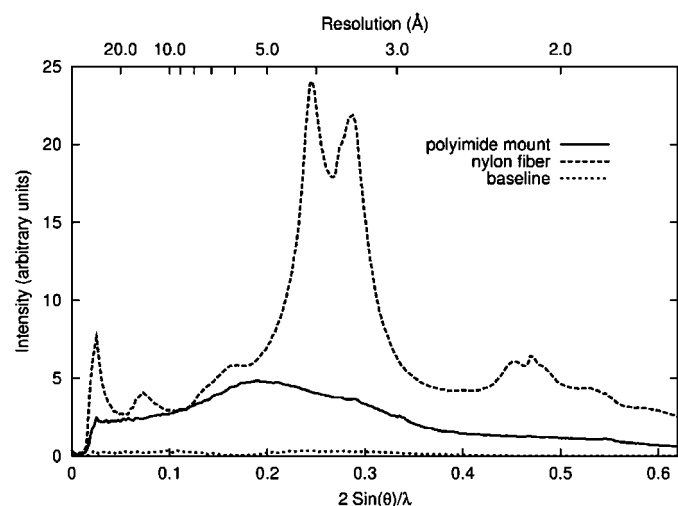


**Figure 6**

Diffuse scattering intensity *versus*  $2\sin(\theta)/\lambda$  and resolution for a 20  $\mu\text{m}$  thick nylon loop and a 9  $\mu\text{m}$  thick polyimide mount when illuminated using a 12.7 keV X-ray beam focused to a 10  $\mu\text{m}$  spot. For the nylon loop, the spot was focused on the middle of the nylon line and for the polyimide film the spot was focused normal to the plane of the film.

submerged in crystal-containing drops, simplifying crystal retrieval. They do not collapse during 'annealing' or 'tempering' procedures used to improve diffraction quality, and show no evidence of mosaicity broadening due to flutter in the cryostream.

Finally, we note that these microfabricated mounts should be more generally useful for small crystals of all kinds, both organic and inorganic. For 'dry' crystals the wicking hole can be eliminated and crystals can be firmly attached using glue or grease, or using a small drop of an ethyl cellulose–ethyl acetate mixture, which can be washed away after data collection.

### 5. Conclusion

We have demonstrated a new approach to mounting crystals for macromolecular cryocrystallography that maintains the many advantages of the nylon loops now in wide use and at the same time resolves most of their deficiencies. Microfabricated polyimide film sample mounts are better suited to handling the very small crystals that can now be characterized at state-of-the-art synchrotron beamlines and that are being produced in abundance *via* automated crystallization at structural genomics centers. These mounts should simplify automation of X-ray data collection and are better suited than existing alternatives for automated crystal retrieval from liquid droplets. Because their fabrication is based on standard microelectronics industry processes, these mounts should be easy and inexpensive to produce in quantities of millions per year, which will soon be required by worldwide structural genomics efforts. They should be more generally useful for small organic/inorganic crystals of all sorts, and especially those of small organic/biological molecules that benefit from cryo-cooling for X-ray data collection.

We wish to thank Tom Ellenberger for pointing out the need for improved ways of mounting small crystals; Katarina Cicak and Mike Skvarla for advice on fabrication methods; Sergei Kriminski for assistance in evaluating prototypes; Christian Riekkel and David Flot for help in data collection at ESRF; and David Schuller and the other staff of the Macromolecular Diffraction Facility (MacCHESS) at the Cornell High-Energy Synchrotron Source (CHESS) for useful feedback. This work was supported by the NIH (R01 GM65981-01) and by NASA (NAG8-1831). Microfabrication was performed at the Cornell Nano-Scale Science & Technology Facility (a member of the National Nanofabrication Users Network) which is supported by the National Science Foundation under Grant ECS-9731293, its users, Cornell University and Industrial Affiliates. CHESS and MacCHESS are respectively supported by the National Science Foundation (DMR 97-13424) and by the NIH through its National Center for Research Resources (RR-01646).

### References

- Garman, E. (1999). *Acta Cryst.* **D55**, 1641–1653.  
Garman, E. F. & Schneider, T. R. (1997). *J. Appl. Cryst.* **30**, 211–237.  
Hope, H. (1988). *Acta Cryst.* **B44**, 22–26.  
Hope, H. (1990). *Ann. Rev. Biophys. Biophys. Chem.* **19**, 107–126.  
Hope, H., Frolow, F., Von Böhlen, K., Makowski, I., Kratky, C., Halfon, Y., Danz, H., Webster, P., Bartels, K. S., Wittmann, H. G. & Yonath, A. (1989). *Acta Cryst.* **B45**, 190–199.  
Inagaki, N., Tasaka, S. & Hibi, K. (1992). *J. Polym. Sci. Part A Polym. Chem.* **30**, 1425–1431.  
Kriminski, S., Caylor, C. L., Nonato, M. C., Finkelstein, K. D. & Thorne, R. E. (2002). *Acta Cryst.* **D58**, 459–471.  
Kriminski, S., Kazmierczak, M. & Thorne, R. E. (2003). *Acta Cryst.* **D59**, 697–708.  
Parkin, S. & Hope, H. (1998). *J. Appl. Cryst.* **31**, 945–953.  
Rodgers, D. W. (1994). *Structure*, **2**, 1135–1140.  
Teng, T. Y. (1990). *J. Appl. Cryst.* **23**, 387–391.  
Yeh, J. I. & Hol, W. G. J. (1998). *Acta Cryst.* **D54**, 479–480.